The fracture behavior of rock salt under present gas pressure in mechanical extension experiments

Lukas Baumgärtel
Leibniz University Hannover, Hannover, Germany

Feline Körner
Leibniz University Hannover, Hannover, Germany

ABSTRACT: The storage of large quantities of energy sources (e. g. natural gas or hydrogen) in rock salt caverns has regained particular importance in today's world. Therefore, the geomechanical design of caverns in rock salt formations is necessary to ensure a safe but also economic operation. Special attention has to be paid to the gas withdrawal phases and the processes resulting for the surrounding rock mass. When the stresses inside the rock fall below the internal gas pressure, effective tensile stresses can cause the development of infiltration fractures.
A special triaxial cell was developed for the laboratory study of such stress states in rock salt. Cylindrical hollow rock salt test specimens are loaded mechanically with an axial, circumferential and internal gas pressure. The axial stress reduction leads to a rupture at different stress differences between axial and gas pressure which shows dependencies on the initial pressure state and temperature.

Keywords: energy storage, rock salt cavern, infiltration fractures, laboratory testing.

1 INTRODUCTION

The use and operation of underground storage caverns in rock salt allows the storage of large volumes of gases and oil. Considering the operating parameters defined by the rock mechanical dimensioning, underground storage caverns can be used for seasonal storage or individual scenarios for gas. The injection and withdrawal of the energy carrier is limited by a defined minimum and maximum internal pressure. Within these limits, gas can be withdrawn or stored at a certain rate, which is also limited to a maximum rate (Zapf et al., 2019). The three operating parameters mentioned above depend in particular on the mechanical and thermal behavior of the surrounding rock salt rock mass and are influenced by the thermodynamics of the storage medium.

The thermo-mechanical calculation of the design load case for an underground gas storage cavern is performed to ensure a flexible and safe operation from a geomechanical point of view. Especially the gas withdrawal phase has to be investigated in more detail, as the prevailing gas pressure in the cavern can get in amount higher (more compressive) than the absolute minimum principal rock stress measured at the wall of the cavern. This can lead to fractures in the rock mass if the effective tensile

strength of the rock mass is exceeded. Such stress conditions during conventional and economical operation are unavoidable (Berest et al., 2012; Zapf et al., 2019).

The following criterion describes the stress state at which infiltration fractures can still be avoided, which could be violated in particular during the gas withdrawal phase:

$$|\sigma_{min}| + \beta_{eff}^{T} > |p_i| \quad (1)$$

where σ_{min} describes the smallest principal compressive stress, p_i the internal cavern pressure and β_{eff}^{T} the effective tensile strength of the material. This formula is valid only if there are no absolute tensile stresses at the considered point of the rock mass.

Zapf et al. (Zapf et al., 2019) conservatively assume that the fracture initiation and propagation in the surrounding rock occurs as soon as the vertical rock stress is smaller (less compressive) than the prevailing internal pressure. An indirect tensile strength for rock salt is not considered. Djizanne et al. (Djizanne et al., 2012) also demand that no effective tensile stresses should occur and thus no indirect tensile strength should be assumed.

Triaxial extension tests under applied internal gas pressure (see Figure 1 for an example) were performed by our Institute, focusing on the magnitude of the stress difference between reduced axial pressure and gas pressure. It is shown that fracturing of salt rock occurs under effective tensile stresses as soon as the gas pressure is 1.0-4.0 MPa larger than the absolute minimum stress component (Baumgärtel et al., 2022; Rokahr et al., 2021; Zapf et al., 2021).

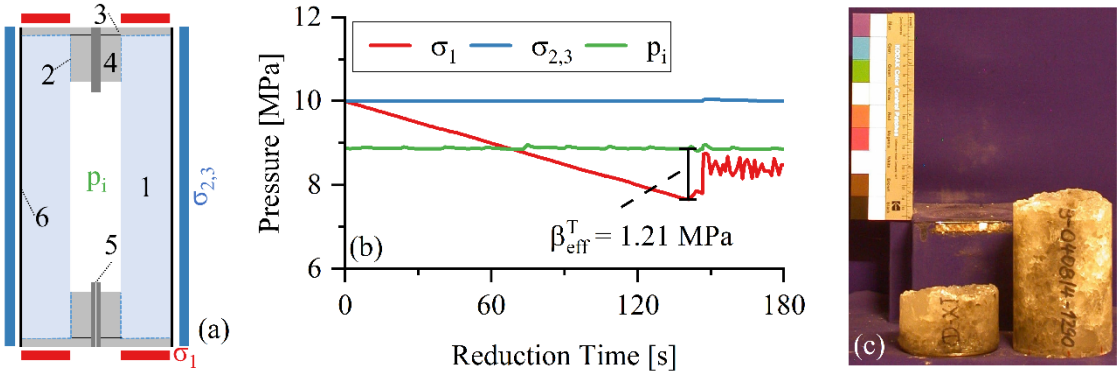

Figure 1. (a) Experimental setup (for description see chapter 2), (b) procedure and (c) result of a laboratory experiment (described in (Baumgärtel et al., 2022)).

Other laboratory studies on the fracture behavior of rock salt at existing effective tensile stresses also indicated a stress difference of 1.5 MPa (Düsterloh, 2009) or 2.0 MPa (Minkley et al., 2013; Minkley et al., 2015) between hydraulic pressure (using oil as pressure medium) and minimum rock pressure.

Furthermore, the method of hydraulic fracturing makes use of the fact that the rock fractures as soon as the hydraulic pressure exceeds the minimum rock pressure by a certain magnitude. Kiersten (Kiersten, 1983) gave stress differences as a function of the applied pressure injection rate for his hydraulic fracturing tests performed on rock salt. Up to a certain critical limit, the values range between 2 and 4 MPa at different boundary stresses. If the determined pressure injection rate is exceeded, the stress difference increases linearly with the logarithmically increasing pressure injection rate. Due to the non-elastic behavior of rock salt, breakdown pressures in hydro fracturing experiments are also dependent on the previous loading time and history as well as the magnitude of confining pressure (Boyce et al., 1984). Schlüter (Schlüter, 1986) determined in his laboratory tests that the breakdown pressure decreases slightly in a linear relationship with increasing test temperature. Furthermore, long-time tests were carried out to show the effects of a constant frac medium overpressure over a longer period of time. It was found that higher confining pressures result in higher hydraulic tensile strength over time. For a confining pressure of p_m = 10.0 MPa, a hydraulic tensile strength T = 2.1 MPa is obtained, and for p_m = 20.0 MPa it is 2.9 MPa.

2 EXPERIMENTAL SETUP

For the investigation of the fracture behavior of rock salt under effective tensile stresses in the laboratory, mechanical triaxial extension tests are carried out under internal gas pressure. For this purpose, cylindrical hollow test specimens (see Figure 1a, no. 1) made of rock salt with a height of 180 mm, an outer diameter of 90 mm and an inner hole with an inner diameter of 30 mm are sampled. Before installation in the triaxial cell, the specimens are bonded at the bottom and top with two-component epoxy resin adhesive (no. 2, blue dashed lines) to a 5 mm height steel plate (no. 3) and a steel plug (no. 4), which has 30 mm in diameter and 30 mm in height, sealing the sample as well. The two steel components are drilled and threaded in the center to allow gas to enter the hollow space through a perforated screw (no. 5) from the bottom of the specimen. An upper screw and the lower gas screw fix the specimen to the pressure plates and create a rigid connection between pressure plate and specimen to allow extension of the sample. Furthermore, the specimen is covered with a nitrile rubber sleeve (no. 6) from the outside to prevent hydraulic oil (for regulating the circumferential pressure) from the triaxial cell from penetrating into the specimen.

Three LVDTs are mounted in 120-degree angles to accommodate the axial displacements between the upper and lower pressure plates. The circumferential displacements at the center of the specimen are measured with a roller chain. Additionally, a temperature sensor is attached outside the nitrile rubber sleeve and is thus located in the hydraulic oil. Furthermore, a permanent acoustic emission sensor is installed in the lower pressure plate. Signal conditioning takes place at 50 Hz with a 1-channel system (ASCO-DAQ, Vallen GmbH, Germany). The experimental temperature is generated with a heating sleeve surrounding the triaxial cell.

3 EXPERIMENTAL PROCEDURE

After the test specimen has been installed in the triaxial cell, the surrounding hydraulic oil and thus the test specimen are heated to the intended test temperature overnight. After the test temperature has been reached, the axial, circumferential and gas pressures are increased to the initial pressure level at a specific pressure rate (loading phase). The test specimen is then subjected to a constant load and temperature for two hours (compaction phase). The background to this is a desired initial compaction of the specimen and leveling of the target temperature, as it rises slightly due to pressure increase. The specimen is then unloaded in the axial direction (pressure-controlled) until the specimen ruptures. This can be assumed as soon as the displacement increases strongly in the negative direction.

A total of four experimental designs, each one with two individual experiments, were performed for this paper. The pressure loading rate or axial pressure unloading rate in the respective phases were 1.0 MPa min^{-1}. The initial pressures in Table 1 indicate the target pressures reached after the loading phase, and the temperatures before the loading phase and during the experiment.

Table 1. Experimental designs.

Experiment type / no.	Initial pressure [MPa] σ_1 / $\sigma_{2,3}$ / p_i	Temperature [°C]
1 / 1.1 and 1.2	8.0 / 8.0 / 7.5	30.0
2 / 2.1 and 2.2	8.0 / 8.0 / 7.5	50.0
3 / 3.1 and 3.2	18.0 / 18.0 / 17.5	30.0
4 / 4.1 and 4.2	18.0 / 18.0 / 17.5	50.0

4 EXPERIMENTAL RESULTS

The relevant pressure component in these experiments is the axial stress, which will be reduced and is shown for these eight experiments in Figure 2a. The circumferential stress and the gas pressure are kept at compaction phase level; these are shown for the respective initial stress level in Figure 2a for the ideal case. During the experiments, there are deviations from the intended pressure level,

especially in the case of the gas pressure, but these do not affect the results or the conclusions of this investigation. The decreasing axial pressure, which is also pressure-controlled, is then interrupted after a certain reduction time by a sudden increase, which indicates that the specimen has been ruptured. It can also be seen that the specimen failure is reached later in the experiments with higher initial stresses and that subsequently there is a higher stress difference.

In the next step, the axial strains (elongation = negative, compression = positive), which are set to 0 at the beginning of the reduction time, are shown in Figure 2b. For five experiments (2.2, 3.1, 4.1, 4.2 and 3.2), there is a rapid decrease (elongation) of the displacement value at different times before the rate increases again and the previously observed displacement behavior occurs again (steps in the displacement). Following this, there is a very fast negative displacement in the axial piston of the testing machine, which stops the axial stress reduction due to specimen failure. Two other experiments (1.1 and 1.2) show several such steps of rapid axial strain decrease, other experiment (2.1) none or only a minimal step.

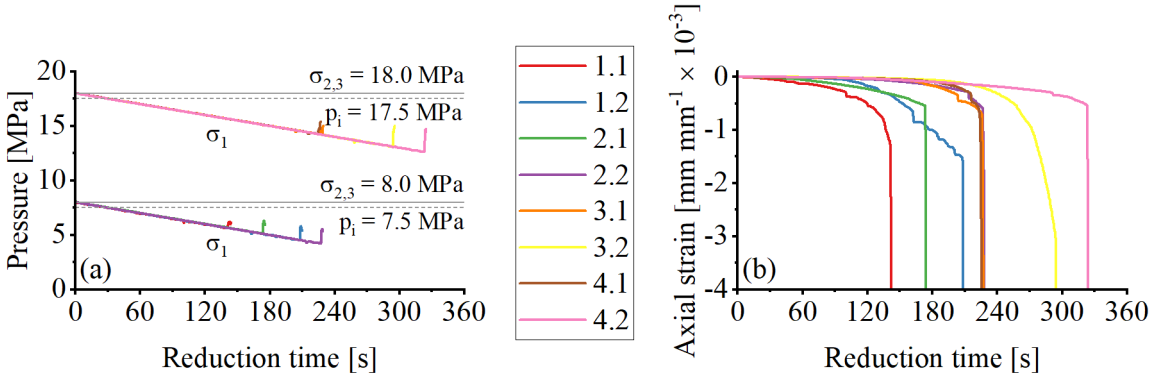

Figure 2. Pressure (a) and axial strain (b) vs. reduction time.

Plotting the axial strain rate also displays this behavior by decreasing in value, meaning faster elongation at these mentioned steps (see Figure 3a). The AE signals above 40 dB recorded during the tests are shown in Figure 3b accumulated from the beginning of the reduction time. It is noticeable that after the change in the axial strain rate has been observed, the AE sensors record only very few to no signals above 40 dB. It can be seen that the slope of the accumulated AE events increases fundamentally as the test duration and unloading progresses after few signals have been sawn.

Furthermore, the sensors in experiments 3.1 and 4.2 do not seem to react as strongly to acoustic emissions, since only a noticeably small number of values are accumulated that are above 40 dB. The assumption is that there was a technical problem which damped the transmission of the electrical waves.

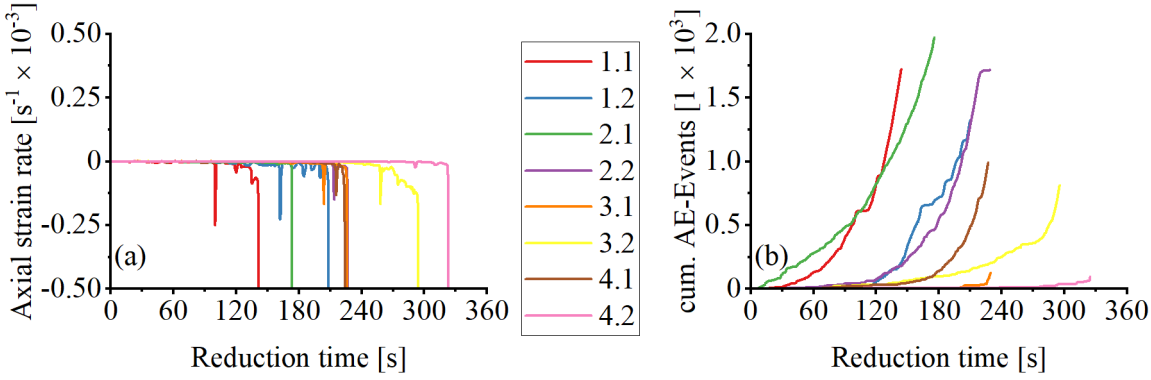

Figure 3. Axial strain rate (a) and accumulated AE-Events (b) vs. reduction time.

Thus, the experimental results show two interesting characteristics, which will be further intensified in the discussion of the results. On the one hand, there is a generally higher fracture stress difference

at higher initial stresses and, on the other hand, several experiments show one or more negative peaks in the axial strain rate (and in other form in the axial strain and the AE signals) shortly before the test is terminated due to specimen failure.

5 DISCUSSIONS AND OUTLOOK

The reduction in axial stress is initially inconspicuous and is accompanied by a slight decrease in axial strain (see Figure 2a). The axial strain rate decreases softly as the axial stress reduction progresses. A drop in the axial strain rate can be noticed before it increases again and approaches around 0 (see Figure 3a). This is often followed by a sharp drop in the axial strain rate and the axial strain.

We assume that the test specimen has a certain infiltration zone into which the gas infiltrates as soon as it is applied. The resulting static friction between the grains decreases with decreasing axial pressure and initially leads to a widening at the weakest part, but not to a rupture of the whole specimen, which was also shown by Schlüter (Schlüter, 1986) in his long-term experiments. It can be expected that there is an increase in the gas volume, when the axial strain rate decreases strongly. There are no noticeable fluctuations in the gas pressure, as it is pressure-controlled and thus not affected by the change of the measured deformation values in axial direction. The change in gas volume can therefore be considered very small, which cannot be measured with the current experimental setup.

After the changes in the axial strain rate, no or only a few AE signals are recorded, and the specimen seems to relax (see Figure 3b). This relaxation can also be seen in the axial strains of the various experiments. The described observations also support the hypothesis that after initial fractures and pathways have been created, the specimen first relaxes and no further fractures are developed before it rapidly experiences further extension loads. To quantify this phenomenon, on the one hand, flow measurements of high accuracy or measurement of the gas pressure drop with a closed gas system would be necessary. These could measure, for one thing, the gas required to maintain the targeted pressure or, in the case of a closed system, the gas pressure drop due to volume increase.

The measured stress differences vary within an initial stress level and show fundamental differences for both initial stress levels considered (see Figure 4).

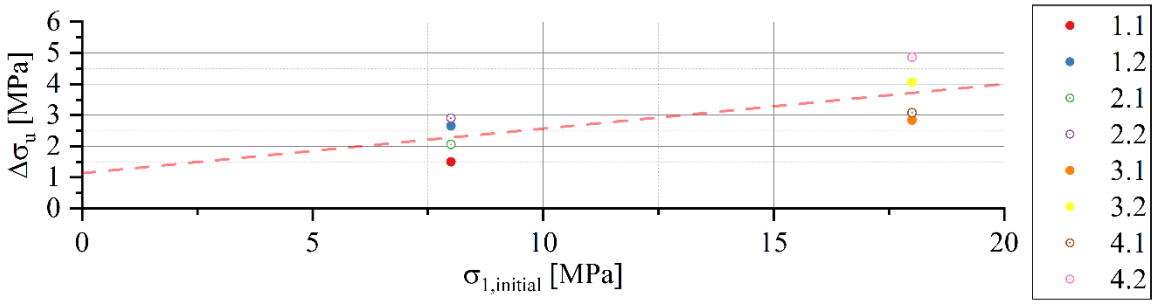

Figure 4. Stress difference $\Delta\sigma_u$ vs. the initial axial stress σ_1 (equal to circumferential stress $\sigma_{2,3}$) of the individual experiments (filled symbols represents 30 °C test temperature, unfilled symbols represents 50°C) including a first linear approximation (red dashed line).

A maximum stress difference between axial and gas pressure of 2.91 MPa for the initial stress level of 8.0 MPa and of 4.87 MPa for the initial stress level of 18.0 MPa is measured. The lower limit is calculated to be 1.50 MPa for experiment 1.1 and 2.84 MPa for experiment 3.2. It can thus be seen, that when the evaluated stress differences are linearly approximated as a function of the initial stress, without taking into account the different temperatures, a slight slope can be expected as the initial stress increases.

For a more accurate approximation, more data must be generated for different initial stress levels. In particular, the investigation of the stages in between the levels presented here gives further information about the fracturing behavior in typical stress ranges of rock stresses in underground

cavern areas. Additional consideration of a lower bound for initial stresses can provide information on the range to which infiltration fractures can still occur. Furthermore, the observed decreases in axial strain and strain rate need to be investigated further as well as the processes at this time inside the test specimen.

ACKNOWLEDGEMENT

The presented work was carried out within the framework of the research project 'LARISSA', which is funded by the Federal Ministry for Economic Affairs and Climate Action (BMWK) of Germany within the framework of the 7th Energy Research Programme (FKZ: 03EI3028).

REFERENCES

Baumgärtel, L., Körner, F., & Leuger, B. (2022). Special Triaxial Experiments on the Fracture Behavior of Hollow Rock Salt Specimens. In American Rock Mechanics Association (Chair), *56th U.S. Rock Mechanics/Geomechanics Symposium,* Santa Fe, New Mexico, USA.

Berest, P., Djakeun-Djizanne, H., Brouard, B., & Hévin, G. (2012). Rapid Depressurizations: Can they lead to irreversible damage? In Solution Mining Research Institute (Chair), *SMRI Spring 2012 Technical Conference,* Regina, Saskatchewan, Canada.

Boyce, G., Doe, T., & Majer, E. (1984). Laboratory hydraulic fracturing stress measurements in salt. *Rock Mechanics in Productivity and Protection*, 95–102. https://escholarship.org/uc/item/8vx7d6w2

Djizanne, H., Berest, P., & Brouard, B. (2012). Tensile effective stresses in hydrocarbon storage caverns. In Solution Mining Research Institute (Chair), *SMRI Fall 2012 Technical Conference,* Bremen, Germany.

Düsterloh, U. (2009). Geotechnische Sicherheitsnachweise für Hohlraumbauten im Salinargebirge unter besonderer Berücksichtigung laborativer Untersuchungen: Ein Beitrag zum Nachweis von Standsicherheit und Barrierenintegrität für untertägige Abfallentsorgungsanlagen und Hohlraumbauten des salinaren Berg- und Kavernenbaus [Habilitation Thesis]. Technische Universität Clausthal-Zellerfeld, Clausthal-Zellerfeld.

Kiersten, P. (1983). Das Hydrofrac-Verhalten von Steinsalz in Abhängigkeit von der Probeneinspannung, der Druckrate, der Flüssigkeitsviskosität und der Standdauer [Dissertation]. Technische Universität Clausthal, Clausthal-Zellerfeld.

Minkley, W., Brückner, D., Knauth, M., & Lüdeling, C. (2015). Integrity of saliferous barriers for heat-generating radioactive waste - natural analogues and geomechanical requirements. In L. Roberts, K. Mellegard, & F. Hansen (Eds.), *Mechanical Behaviour of Salt VIII* (Vol. 8, pp. 159–170). CRC Press LLC.

Minkley, W., Knauth, M., & Brückner, D. (2013). Discontinuum-mechanical behaviour of salt rocks and the practical relevance for the integrity of salinar barriers. In American Rock Mechanics Association (Chair), *47th US Rock Mechanics / Geomechanics Symposium,* San Francisco, California, USA.

Rokahr, R. B., Zapf, D., Leuger, B., & Siemann, L. (2021). Laboruntersuchungen von thermisch-induzierter und gasdruckgetriebener Rissbildung im Salzgestein (La-thi-ga): Final report. https://doi.org/10.2314/KXP:1775726282

Schlüter, K. (1986). Das Hydrofrac-Verhalten von Salzgesteinen in Abhängigkeit von der Salzart, Einspannung und Druckerhöhungsrate [Dissertation]. Technische Universität Clausthal, Clausthal-Zellerfeld.

Zapf, D., Leuger, B., Baumgärtel, L., & Körner, F. (2021). Laborative und numerische Untersuchungen zu Infiltrationsrissen in der Umgebung von Salzkavernen. *Erdöl Erdgas Kohle*, *137*(12), 17–25.

Zapf, D., Rokahr, R. B., Leuger, B., & Yildirim, S. (2019). Influence of Infiltration Fractures on the Stress Field in the Vicinity of Gas Storage Caverns in Rock Salt. In Solution Mining Research Institute (Chair), *SMRI Spring 2019 Technical Conference,* New Orleans, Louisiana, USA.